

Experimental study of the expansion mechanism of the solid-state plasma in silicon

T. X. Hoai, P. H. Duong, D. X. Thanh, T. H. Nhung, and H. K. Phan

Institute of Physics Center for Scientific Research of Vietnam, Nghiado, Tuliem Hanoi, Vietnam

(Received 3 September 1987; revised manuscript received 5 September 1989)

The spatial expansion of the electron-hole plasma in surface-excited silicon is investigated with the use of a transient photoconductive time-of-flight technique on the subnanosecond time scale. We find that the expansion is faster at high excitation levels than it is at low excitation levels. The experiments indicate that there are two expansion mechanisms, diffusion and drift, with the latter dominant at high excitation levels. The drift velocity is estimated to be near the sound velocity, that is, in the range $(1-3) \times 10^5$ cm/s.

In the last five years the transport properties of high-density electron-hole plasmas created by intense laser excitation in semiconductors have become the subject of controversy. Beginning with the study of the mechanism of pulsed-laser annealing (PLA) in semiconductors, it has been suggested that the plasma produced by nanosecond pulses will be confined near the excitation surface, softening the lattice and causing the annealing process.¹ Another viewpoint² is that the PLA is mainly a thermal process in which the plasma is not confined, but is expanding into the crystal.

While the thermal mechanism of PLA is generally accepted, recently radically different results concerning the motion of the electron-hole plasma have been reported: Using recombination luminescence spectra and fits of the luminescence emission line using a single Fermi energy, Forchel and co-workers^{3,4} calculated the plasma density and found that it was not consistent with the spectral position of the plasma resonance. In order to explain this anomaly, they proposed that the carriers in the plasma were drifting away from the excitation point at a velocity comparable to the Fermi velocity; that is, at 10^7 cm/s at low temperatures. The results of luminescence time-of-flight measurements at low temperatures⁵ seem to favor this assumption of a high-speed electron-hole plasma. On the other hand, Wolfe and co-workers,⁶ by combining time-resolved spectroscopy with spatial imaging, have come to the conclusion that, on a several-nanosecond time scale, the plasma generated at the surface of the crystal is either stationary or diffusing slowly into the bulk. They obtained a maximum plasma velocity of 1.7×10^5 cm/s at 25 K, which is even slower than that observed for the electron-hole liquid at 10 K.

High-speed electron-hole plasmas have also been observed in several other materials,⁷⁻¹⁰ but the experimenters have made various interpretations of the results. For example, Auston and co-workers⁷ explained the high-speed motion of the electron-hole plasma in Ge as the result of an increase in the ambipolar-diffusion constant by a factor of at least 3.5 times the value for a low-density plasma. In CdS (Ref. 8) an expansion velocity of 10^8 cm/s, requiring an enhancement of the diffusion coefficient by a factor of 10^6 , has been proposed. A theoretical study¹¹ predicts an increase of the diffusion

coefficient in dense electron-hole plasma of about 1 order of magnitude in polar semiconductors.

In this paper we report the first measurements of solid-state plasma expansion by means of a photoconductive (PC) time-of-flight technique as well as by a measurement of a transient photomagnetolectric effect (PME) at room temperature. Doing the experiments at room temperature has the advantage that, unlike low-temperature experiments, the electron-hole plasma is in the same phase at all the excitation levels studied. The photoelectric time-of-flight technique provides significant advantages over luminescence spectroscopy, which has proven to be a valuable tool in the characterization of the solid-state plasma at low temperatures, but which cannot be applied at room temperatures for an indirect-band-gap semiconductor like silicon.

The key feature of the PC technique is the development of an ultrafast photoconductivity detector directly on one surface of the silicon sample. In our experiments, we have fabricated a surface metal-oxide-silicon-oxide-metal subnanosecond detector using the back surface of the silicon sample as the substrate for the detector. On this surface, a thin, very uniform oxide layer was grown by thermal oxidation. Aluminum strip-line electrodes were fabricated on top of this oxide layer by vacuum evaporation. As described by Thaniyavarn *et al.*,¹² the metal-oxide-silicon-oxide-metal junction in this device is basically composed of two back-to-back metal-insulator-semiconductor tunnel diodes. When a dc bias is applied to this structure, a high electric field develops in the totally depleted region immediately below the surface. Photogenerated electron-hole pairs created in this high-field region drift apart. The holes drift to the cathode, inducing more electrons to tunnel from the aluminum cathode, providing a current gain. The time for photo-carriers to drift to the cathode is very short and does not significantly affect the temporal resolution of the detector: With a gap between the cathode and anode of $20 \mu\text{m}$ and a bias of 5 V, the transit time of the carriers across the gap is approximately 0.9 ns. Thus the resolution of the detector is limited by the response time of the current detector (3.5 ns) and the laser-pulse duration (up to 5 ns). We observe a long-time tail in the reference signal (see Fig. 1), which is probably due to traps on the surface,

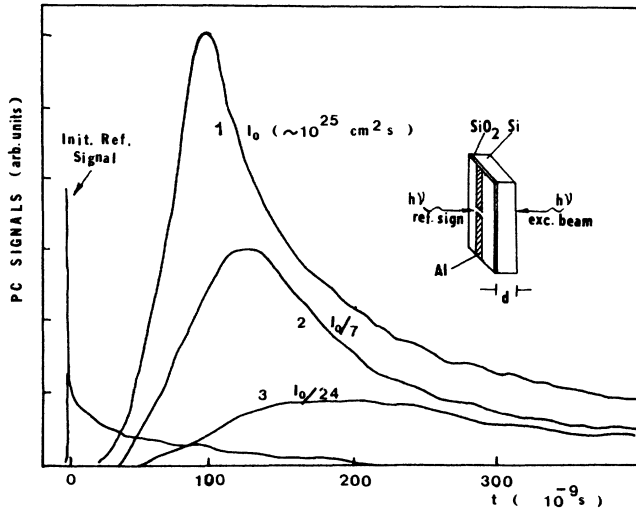


FIG. 1. Time evolution of the PC signal at different levels of excitation.

since its height saturates quickly with increasing levels of excitation.

Carrier pairs are excited at the front surface of the sample by a short laser pulse from either a N_2 laser (0.9-ns pulse) or a dye laser (5-ns pulse). To observe the resulting time-dependent change in the photoconductivity on the back surface, it was necessary to locate the laser spot in the front surface exactly opposite the electrodes on the back surface. When the photoexcited electron-hole plasma propagates to the back surface of the sample, a photoconductive current is observed through the metal electrodes. We determine the time of flight of the carriers from the time dependence of this photoconductive current as shown in Fig. 1. Clearly, for high excitation levels the expansion of the plasma is faster. To analyze the data in Fig. 1, we use a generalized diffusion equation with a drift term that takes the following form:

$$\frac{\partial n(x,t)}{\partial t} = D \frac{\partial^2 n(x,t)}{\partial x^2} - v \frac{\partial n(x,t)}{\partial x}. \quad (1)$$

At high excitation levels, v is assumed to be dependent on the excitation intensity, but position independent within an expansion distance comparable to the mean free path of the carriers. For the PC signal we model the system as a one-dimensional semi-infinite sample with the surface detector at position $x = d$. The duration of the excitation pulse and the depth of the absorption layer are negligible compared with the measured time of flight and the thickness of the sample, respectively. Thus the signal at $x = d$ is proportional to the value of the solution to the generalized diffusion equation:

$$n(x=d, t) = \frac{N_0}{Dt} \exp \left[-\frac{(d-vt)^2}{4Dt} \right]. \quad (2)$$

The peak position t_m in the time-of-flight signal is the time at which this quantity is maximum:

$$t_m = \frac{D}{v^2} \left[\left(\frac{v^2 d^2}{D^2} + 1 \right)^{1/2} - 1 \right]. \quad (3)$$

When $v = 0$ (at low excitation levels), this reduces to the diffusive form $t_m = d^2/2D$. In Fig. 2 we show the time of flight of the plasma as determined from the positions of the peaks in curves in data like that of Fig. 1 for a range of excitation levels and for two sample thickness. The velocities v_{\max} shown in the figure are computed from (3) using the known value of the diffusion constant. At low excitation levels the expansion speed of the plasma is almost constant. In the thick sample, the high-density plasma cannot reach the detector, so that the maximum speed is smaller.

To gain further insight into the plasma-expansion mechanism, we have performed transient photomagneto-electric (PME) short-circuit (SC) current measurements on the same samples on a subnanosecond time scale. The PME effect may be described as the Hall effect associated with the expansion into the crystal of the electron-hole plasma produced optically at the sample surface.¹³ The transient from the PME SC current is very sensitive to such expansion parameters of the plasma as the diffusion coefficient and the drift velocity.

The experimental geometry is indicated in the inset of Fig. 3. The setup is similar to that used in the photoconductive measurements described above, except that a magnetic field B of 5 kG is applied parallel to the surface of the sample which is excited optically and the PME current is monitored parallel to the excited surface and

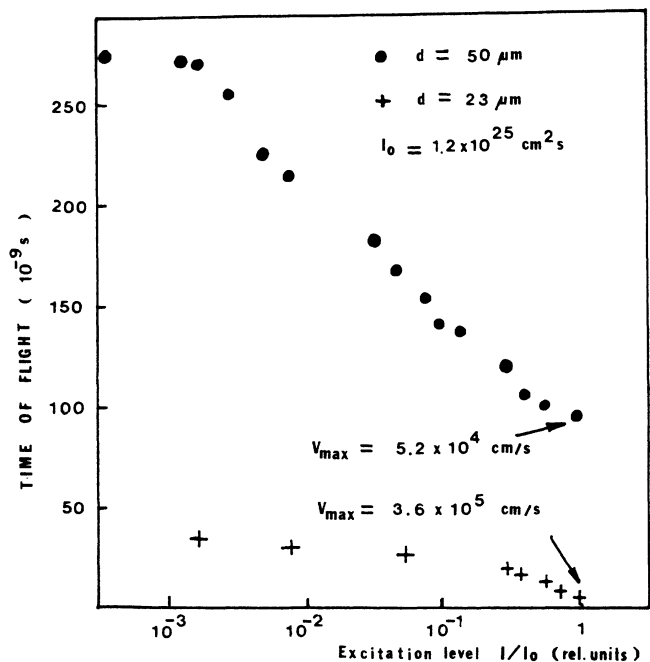


FIG. 2. Time of flight vs excitation level at different sample thicknesses d .

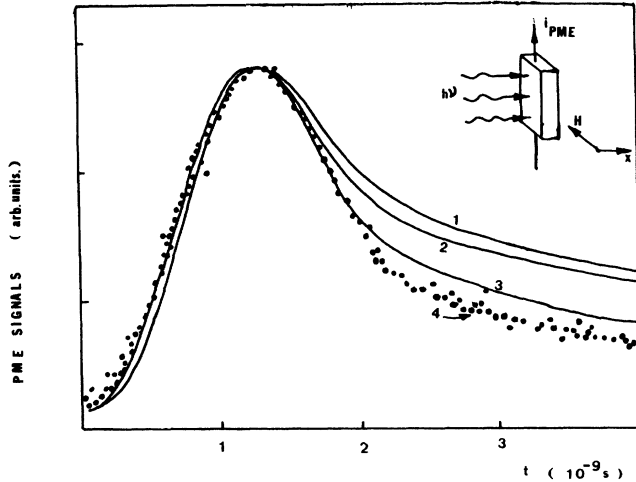


FIG. 3. Time evolution of the PME SC current. The dotted curve is the experimental data (marked 4). The theoretical curves are labeled 1 ($D = 100 \text{ cm}^2/\text{s}$; $v = 0$), 2 ($D = 2000 \text{ cm}^2/\text{s}$; $v = 0$), and 3 ($D = 100 \text{ cm}^2/\text{s}$; $v = 10^5 \text{ cm/s}$).

perpendicular to the magnetic field. The samples were high-purity silicon slabs ($0.1 \times 0.5 \times 0.015 \text{ cm}^3$). Photoconductive measurements were carried out on the same samples in the same configuration and showed that bulk and surface recombination could be neglected. The excitation source was a N_2 transversely excited atmospheric laser with a full band at half maximum pulse width of about 0.9 ns. To separate the PME SC current signals from the background noise, we averaged digitized data from many pulses by use of a sampling head on-line to a microcomputer. We subtracted the average noise signal and subtracted the two averaged signals with opposite directions of the magnetic field in order to eliminate all the magnetic-field-independent parasite signals. In Fig. 3 we show a typical PME SC current pulse taken at an excitation level close to the irradiation-damage threshold for silicon.

To describe the temporal evolution of the PME current theoretically, we note that the magnetic field is small and, by independent measurement, the surface recombination rate is negligible ($< 10^3 \text{ cm/s}$), while the carrier lifetime is large ($\approx 1 \mu\text{s}$) compared with the excitation-pulse time.

Under these conditions, the PME SC current is proportional to the magnetic field and to the integral $\int j_x dx$ of the current density j_x in the direction x of the incoming light. Assuming the same model (1) for the propagation of carriers, one shows easily that the PME SC current i_D is given by

$$i_D(t) \propto \int j_x(x,t) dx = Dn(x,t) \Big|_{x=0} + v \int_0^x n(x,t) dx. \quad (4)$$

This depends only on $n(x,t)$, which is obtained by solving Eq. (1) with the boundary conditions that n have zero gradient at the front surface and value zero at the back surface. Initially, n is supposed to decay exponentially into the semiconductor with a decay length given by the inverse of the optical-absorption coefficient. In most practical cases, the second term in (4) is constant and can be neglected. Finally, we construct the observed signal $i_{\text{PME}}(t)$ by convoluting $i_D(t)$ with a shape function $S(t) = S_0 \sin^2(2\pi t/T)$ characterizing the excitation pulse:

$$i_{\text{PME}}(t) \propto \int_{-\infty}^{\infty} i_D(\tau) S(t-\tau) d\tau. \quad (5)$$

The resulting predicted PME signal is compared with experiment in Fig. 3. In that figure, curve 1 is the solution with $v = 0$ and the reported value of the diffusion constant, while curve 2 has $v = 0$ and a diffusion constant 20 times larger. Curve 3 includes the drift term with $v = 10^5 \text{ cm/s}$. One sees that adding the drift term results in a much better fit with the experimentally observed current (curve 4). The velocity needed to describe the time dependence of the PME current is consistent within experimental uncertainties with the maximum average velocity measured in time-of-flight experiments.

In conclusion, we have shown that, while at low densities the electron-hole plasma can be described by a diffusion equation, at higher densities this is not possible, and the data are consistent with a plasma described by an equation including diffusion and drift, with a drift velocity near the sound velocity.

We wish to thank N. D. Hung, T. P. Dat, and co-workers for helping in the construction of laser sources. B. Huy and T. Ha are thanked for assistance in the preparation of samples. We are grateful to J. W. Halley for discussion and a critical reading of the manuscript.

¹J. A. Van Vechten, and A. D. Compaan, *Solid State Commun.* **39**, 867 (1981).

²M. Combescot, *Phys. Lett.* **85A**, 308 (1981).

³G. Mahler, G. Maier, A. Forchel, B. Launrich, H. Sanwald, and W. Schmid, *Phys. Rev. Lett.* **47**, 1855 (1981).

⁴A. Forchel, H. Schweizer, and G. Mahler, *Phys. Rev. Lett.* **51**, 501 (1983).

⁵A. Forchel *et al.*, in *Proceedings of the 17th International Conference on the Physics of Semiconductors*, edited by T. P. Chadi and W. A. Harrison (Springer-Verlag, New York (1984), p. 1285.

⁶F. M. Steranka and J. P. Wolfe, *Phys. Rev. Lett.* **53**, 2181 (1984).

⁷D. H. Auston and C. V. Shank, *Phys. Rev. Lett.* **53**, 2181 (1984).

⁸A. Cornet *et al.*, in *Proceedings of the 3rd International Conference on Picosecond Phenomena*, edited by K. B. Eisenthal, R. M. Hochtrasser, W. Kaiser, and A. Laubereau (Springer-Verlag, New York, 1982), p. 364.

⁹K. M. Romanek, H. Nather, J. Fisher, and E. O. Gobel, *J. Lumin.* **24/25**, 585 (1981).

¹⁰K. Kempf and C. Klingshirn, *Solid State Commun.* **49**, 23 (1984).

¹¹A. R. Vasconcellos and R. Luzzi, in Ref. 5, p. 1341.

¹²S. Thaniyavarn and T. K. Gustafson, in Ref. 8, p. 137.

¹³W. van Roosbroeck, *Phys. Rev.* **101**, 1713 (1956).